Structural Engineering and Mechanics, Vol. 10, No. 1 (2000) 27-36
DOI: http://dx.doi.org/10.12989/sem.2000.10.1.027

Member capacity of columns with semi-rigid end conditions in Oktalok space frames

Xiao-Ling Zhao†

Department of Civil Engineering, Monash University, Clayton, VIC 3168, Australia

Peter Lim‡ and Paul Joseph‡†

Spacetech Pty Ltd, Moorabbin, Melbourne, Australia

Yong-Lin Pi‡‡

Department of Civil Engineering, The University of Sydney, Sydney, Australia

Abstract. The Oktalok nodal connection system is an aesthetic and efficient system. It has been widely used throughout Australia. The paper will briefly introduce the concept and application of the Oktalok nodal system. The existing design method is based on the assumption that the joints are pin-ended, i.e., the rotational stiffness of the joints is zero. However the ultimate capacity of the frame may increase significantly depending on the rotational stiffness of the joints. Stiffness tests and finite element simulations were carried out to determine the rotational stiffness of the Oktalok joints. Column buckling tests and non-linear finite element analyses were performed to determine the member capacity of columns with semi-rigid end conditions. A simple formulae for the effective length factor of column buckling is derived based on the above experimental and theoretical investigations.

Key words: buckling; column; semi-rigid joint; space frame; tubes.

1. Introduction

Space frames are widely used all over the world. They can be in different forms, such as planar grid, cylindrical arch, spherical dome and surface of revolution. Different nodal connection systems have been developed for use in space frames. They can be summarised as:

- Oktaplatte system and Mero system in Germany (Makowski 1965)
- Zublin system in Germany (Fastenau 1984)
- Triodetic system in Canada (Fentiman 1966, Vangool and Fentiman 1984)
- Unistrut system in USA (Hsiao 1966)
- Power-Strut system in USA (Gebhardt 1984)

† Senior Lecturer
‡ Director
‡† Senior Engineer
‡‡ Senior Research Fellow

- Octatube system in the Netherlands (Gerrits 1975)
- Gyro system in Czech Republic (Russ *et al.* 1984)
- Mostostal system in Poland (Brodka *et al.* 1984)
- SDC system, Pyramitec system, Tridiatec system and Spherobat system in Poland (Du Chateau 1995)
- NS system in Japan (Iwata *et al.* 1984)
- Ball joint system in Japan (Tanaka 1994)
- Mine-type system in China (Ding *et al.* 1994)
- Nodus system in UK (BSC 1981, Bell and Ho 1984)
- Cubic system in UK (Shanmuganathan and Kubik 1993)

The nodal system discussed in this paper is an Australian designed and manufactured product named "Oktalok". The space frames utilising the Oktalok nodal system have been used throughout Australia and in Thailand and Hong Kong (Spacetech 1995). A list of projects using Oktalok space frames was presented in Zhao *et al.* (1997).

An Oktalok nodal connection consists of 5 parts as shown in Fig. 1. They are:

1. Spherical forged node connector
2. Tapered conical end piece
3. Circular hollow section
4. High strength socket head cap screw fastener
5. Keyhole port for fastener access

The node connector has a maximum of eight members bolted to it, hence the name "Okta" lok. The circular hollow sections are manufactured using a cold-forming process in accordance with the Australian Standard for Structural Steel Hollow Sections AS1163 (SAA 1991).

Structural testing on Oktalok space frames showed that the space frame satisfied the requirement for deflection recovery specified in British Standards (Zhao *et al.* 1997). It was also found that the ultimate capacity of the space frame is much higher than that predicted assuming that the joints are pin-ended, i.e., the rotational stiffness of the joints is zero.

In this paper, stiffness tests are performed to determine the rotational stiffness of the Oktalok

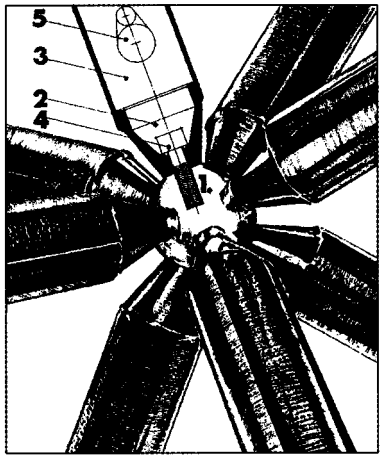

Fig. 1 Components of Oktalok Nodal System

joints. Finite element analysis is carried out to simulate the rotational stiffness of the Oktalok joints. Column buckling tests are performed to determine the member capacity of columns with semi-rigid end conditions. The member buckling capacity is investigated using a non-linear finite element analysis. A simple formulae for the effective length factor of column buckling is derived based on the above experimental and theoretical investigations.

2. Rotational stiffness of the Oktalok joints

2.1. Experimental investigation

Three different sizes of circular hollow sections were used in the stiffness tests. The dimensions and section properties are summarised in Table 1.

Four sets of tests were performed. The specimen labels are listed in column 1 of Table 2. In the label, the first letter S means Stiffness test, followed by the section identification number (S1, S2 and S3), M12 stands for bolt M12, M16 stands for bolt M16. Two specimens were tested for each set of tests.

The stiffness test was designed to isolate the joint as a cantilever and apply a lateral force to generate a moment. The test set up is shown in Fig. 2. Only half of the node was needed, which was bolted to a *L*-plate. The diameter of the node is 109 mm. The rig was fit on a Baldwin testing machine in the Civil Engineering Laboratory at Monash University. Inclinometers were used to measure the rotation angle (ϕ). The moment (M) versus rotation angle (ϕ) curves were recorded. It was found that there are always two slopes (C_1 and C_2) in a moment (M) versus rotation angle (f) curve, as shown in Fig. 3.

The measured average values of rotational stiffness are summarised in Table 2. The adopted values are shown in column 5 of Table 2, as explained in Section 2.2. It can be seen from column 5

Table 1 Dimensions and section properties of circular hollow sections

Section Identification No.	Diameter d (mm)	Thickness t (mm)	Second moment of area I (10^6 mm^4)	Radius of gyration r (mm)
S1	48.3	2.3	0.0881	16.3
S2	42.4	2.0	0.0519	14.3
S3	60.3	2.3	0.177	20.5

Table 2 Specimen labels and measured rotational stiffness

Test Specimens (1)	C_1 (10^3 Nmm/rad) (2)	C_2 (10^3 Nmm/rad) (3)	$(C_1 + C_2)/2$ (10^3 Nmm/rad) (4)	C (adopted) (10^3 Nmm/rad) (5)
SS1M12	21885	6273	**14079**	14079
SS2M12	24098	5964	**15031**	15031
SS3M12	41579	**15529**	28554	15529
SS3M16	54920	**18247**	36584	18247

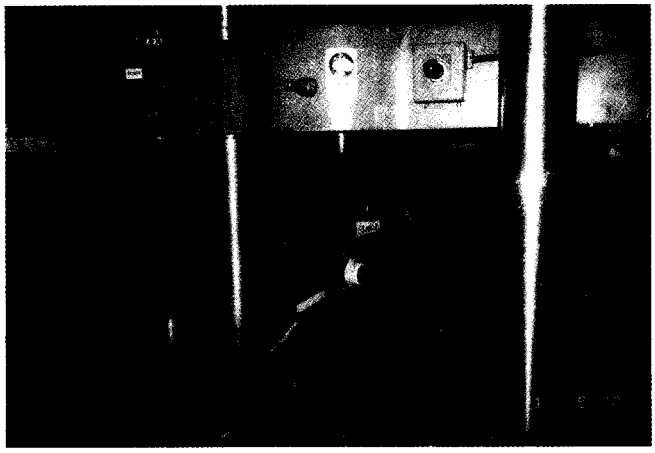

Fig. 2 Set up for stiffness tests

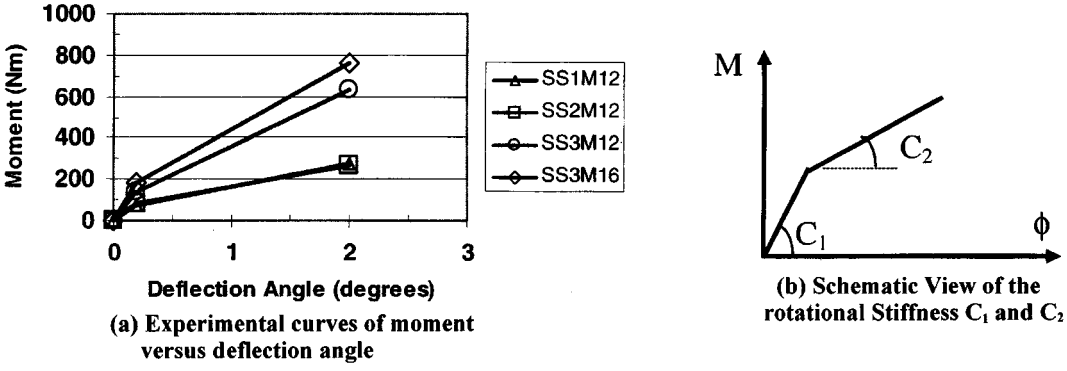

(a) Experimental curves of moment versus deflection angle

(b) Schematic View of the rotational Stiffness C_1 and C_2

Fig. 3 Moment (M) versus rotation angle (ϕ) curve

of Table 2 that the increase in rotational stiffness due to the use of M16 is about 19% (ie. the ratio of 18247 to 15529).

2.2. Finite element simulation

Finite element analysis was carried out to simulate the rotational stiffness of the Oktalok joints. The FE package LUSAS was used. Due to the symmetry in loading and geometry, only half of the structure was modelled. Symmetry boundary condition was applied to all central planes. Fully fixed boundary condition was applied to the end of the bolt. The lower part of the end surface of the cone was restrained in the axial direction. Contact was defined between the surfaces of bolt and cone. Four-node shell elements were used for the circular hollow sections and eight-node brick elements were used for the rest of structure. Typical meshes (undeformed and deformed) are shown in Fig. 4, where (a) shows the mesh including the keyhole and (b) shows the mesh excluding the keyhole for simplicity.

The predicted rotational stiffness from the FE analysis is shown in Table 3. It was found that for SS3M12 yielding of the material occurs when the slope changes from C_1 to C_2. It is more reasonable

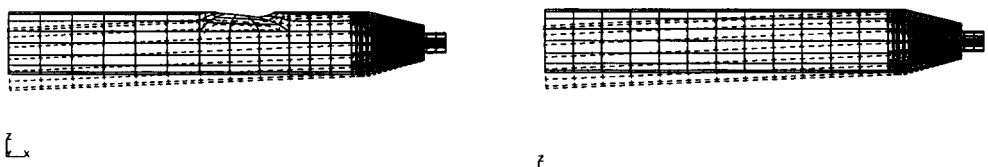

(a) Mesh including the keyhole (b) Mesh excluding the keyhole

Fig. 4 Typical meshes in finite element analysis

Table 3 Predicted values of rotational stiffness

Model of Specimens (1)	C_1 (10^3 mm/rad) (2)	C_2 (10^3 Nmm/rad) (3)	$(C_1 + C_2)/2$ (10^3 Nmm/rad) (4)	C (adopted) (10^3 Nmm/rad) (5)
SS1M12	23401	6875	**15138**	15138
SS2M12 (include keyhole)	25545	6553	**16049**	16049
SS2M12 (exclude keyhole)	25896	6605	**16251**	16251
SS3M12	54264	**16441**	35353	16441

to adopt C_2 as the rotational stiffness for SS3M12, otherwise it may produce an overestimation of rotational stiffness. For SS1M12 and SS2M12, the yielding occurs after the change of slope. It is more reasonable to adopt $(C_1+C_2)/2$ as the rotational stiffness for SS1M12 and SS2M12.

It can be seen that the exclusion of the keyhole in the model only has a minor effect on the rotational stiffness. By comparing column 5 of Table 2 and that of Table 3, the predicted rotational stiffness is about 6.7% on average higher than the tested values. The overestimation may be due to the ideally fixed end condition. The prediction can be considered as satisfactory.

3. Member capacity with semi-rigid end conditions

3.1. Experimental investigation

Three sets of column buckling tests were performed. The specimen labels are listed in column 1 of Table 4. In the label, the first letter C means Column buckling test, followed by the section identification number (S1, S2 and S3), M12 stands for bolt M12. Three specimens were tested for each set of tests.

The column tests were performed in the Baldwin testing machine in the Civil Engineering Laboratory at Monash University. Similar to the stiffness tests, only half nodes are used at the specimen ends, as shown in Fig. 5. The diameter of the node is 109 mm. The length of the column is 2000 mm. The load versus lateral deflection curves were recorded. The average maximum loads obtained in the tests ($P_{max,test}$) are listed in column 4 of Table 4.

Table 4 Specimen labels, test results and comparisons of member capacities

Specimens	Slenderness (L/r)	P_e (kN)	$P_{max,test}$ (kN)	$P_{max,NFE}$ (kN)	$P_{max,C}$ (kN)	$P_{max,NFE}$ /$P_{max,test}$	$P_{max,C}$ /$P_{max,test}$
(1)	(2)	(3)	(4)	(5)	(6)	(7)	(8)
CS1M12	123	43.5	76.6	67.0	67.4	0.875	0.880
CS2M12	140	25.6	48.6	48.7	48.1	1.002	0.990
CS3M12	98	87.4	113.2	112.6	116.2	0.995	1.027
MEAN	–		–	–	–	0.957	0.965
COV	–		–	–	–	0.061	0.065

Fig. 5 Set up for column tests

3.2. Non-linear finite element analysis

A non-linear inelastic finite element analysis (FEA) was carried out to determine the member capacity. The finite element program developed by Pi and Trahair (1994a) was used to calculate the failure load. The analysis considered both geometric and material non-linearity. The finite element program has been successfully applied to steel beams (Zhao *et al.* 1995), beam-columns (Pi and Trahair 1994b) and arches (Pi *et al.* 1995, Pi and Trahair 1996). The geometric imperfection, i.e. the initial lateral deflection at the mid-span, is taken as $L/1{,}000$ corresponding to the fabrication limit specified in SAA (1998), where L is the length of the member. The residual stresses were assumed to vary linearly through the wall thickness of cross section with tension residual stress outside and compression residual stresses inside (Key and Hancock 1993). The maximum residual stress is $0.5\sigma_y$ where σ_y is the measured yield stress. The measured stress-strain curve was used in the analysis to define the material properties.

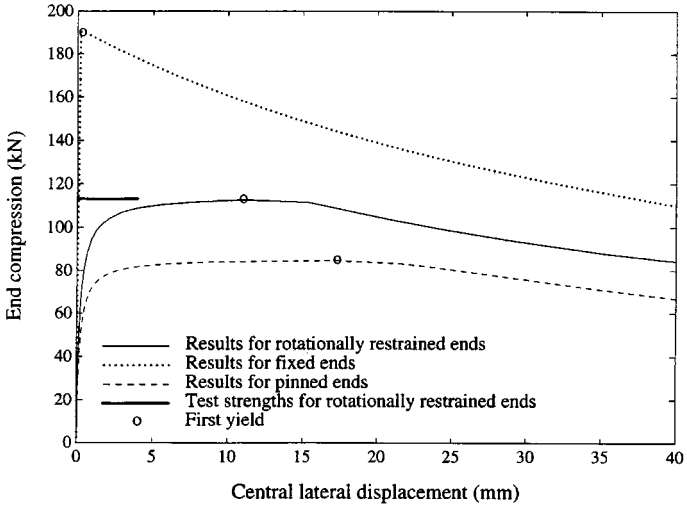

Fig. 6 Non-linear finite element analysis (CS3M12)

The analysis has been performed for CS1M12, CS2M12 and CS3M12. Only the results for CS3M12 are shown in this paper as Fig. 6. The highest curve in Fig. 6 is based on a fixed-end condition, which produces an inelastic buckling behaviour. The lowest curve in Fig. 6 is based on a pin-ended condition, which produces mainly an elastic buckling behaviour. The curve based on the measured rotational stiffness lies in between.

4. Effective length factor of column buckling

4.1. Comparison of member capacities

The predicted maximum loads from the non-linear FE analysis ($P_{max,NFE}$) are compared in Table 4 with the tested values ($P_{max,test}$). The member capacity can also be determined using the restrained-column theory (Bazant and Cedolin 1991), as shown in Eq. (1), i.e., the member is approximated as a column whose ends are restrained against rotation by springs with stiffness C. The predicted member capacities based on the measured rotational stiffness ($P_{max,C}$) are given in Table 4.

$$P_{cr}=\frac{\pi^2 EI}{L^2}\left[\frac{(0.4+\lambda)^2}{(0.2+\lambda)^2}\right] \tag{1}$$

where E is the Young's modulus, I is the second moment of area, L is the length of the member, $\lambda = EI/CL$, and C is the rotational stiffness.

The predicted member capacities shown in Table 4 are in good agreement with tested values.

4.2. Effective length factor of column buckling

The member capacity can be determined using Euler buckling theory as shown in Eq. (2), i.e., the

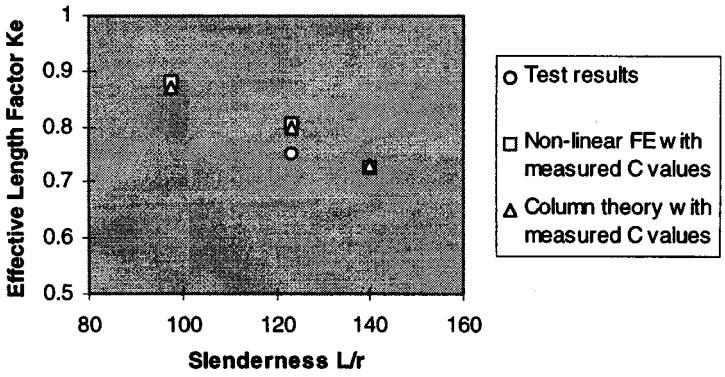

Fig. 7 Effective length factor (k_e) versus column slenderness (L/r)

member is approximated as a column which has a certain buckling length. The reference buckling capacity P_e is listed in column 3 of Table 4. The effective length factor k_e can be obtained from Eq. (3) by using the member capacities listed in columns 4, 5, and 6 of Table 4 as P_{cr}. The values of k_e determined so are plotted in Fig. 7 against the slenderness (L/r).

$$P_{cr}=\frac{\pi^2 EI}{(k_e L)^2}=\frac{1}{k_e^2}\frac{\pi^2 EI}{L^2}=\frac{P_e}{k_e^2} \tag{2}$$

$$k_e=\sqrt{\frac{P_e}{P_{cr}}} \tag{3}$$

A simple expression of k_e in terms of L/r can be derived based on a linear regression analysis in Fig. 7, as shown in Eq. (4).

$$k_e=1.25-\frac{L/r}{267} \tag{4}$$

where $98 \le L/r \le 140$.

It can be seen from Fig. 7 and Eq. (4) that the larger the slenderness of a column, the more increase in column buckling capacity due to the semi-rigid end conditions. It should be noted that Eq. (4) is only valid when both end connections are identical and when side-sway is totally inhibited. More research is needed to study the effect of different end conditions and side-sway on the member capacity of Oktalok space frames.

5. Conclusions

1. The rotational stiffness of the Oktalok joints has been determined using stiffness tests and finite element simulation. The exclusion of keyhole in FE model only has a minor effect on the rotational stiffness. The predicted rotational stiffness is about 6.7% higher than the tested values.

2. The member capacity has been determined using column tests, non-linear finite element analysis and column theory with measured rotational stiffness. The predicted member capacities are in good agreement with tested values.

ASCE, **122**(7), 734-747
Russ, R. *et al.* (1984), "Prefabricated steel space structures designed by Chemoprojekt Prague-CSSR", *Proc. 3rd Int. Conf. on Space Structures,* Elsevier, London, 42-47.
SAA. (1991), "Structural steel hollow sections", *Australian Standard,* AS1163, Standards Association of Australia, Sydney.
SAA. (1998), "Steel Structures", *Australian Standard,* AS4100, Standards Association of Australia, Sydney
Shanmuganathan, S. and Kubik, L.A. (1993), "Optimization of CUBIC space frame structures", *Proc. 4th Int. Conf. on Space Structures,* Thomas Telford, London, 1766-1773.
Spacetech. (1995), "Oktalok Space Frame System", Brochure, Spacetech Pty Ltd, Moorabbin, Victoria.
Tanaka, T. *et al.* (1994), "The strength of ball joints in space trusses-Part III", *Tubular Structures VI,* Grundy, P. *et al.* (Eds), Balkema, Rotterdam, 123-131.
Vangool, W.J. and Fentiman, H.G. (1984), "Triodetic structural frameworks for Les Forges Du Saint-Maurice National Historical Parks-Canada", *Proc. 3rd Int. Conf. on Space Struct.,* Elsevier, London, 994-997.
Zhao, X.L., Hancock, G.J., Trahair, N.S. and Y.L. Pi. (1995), "Lateral buckling of cold-formed RHS beams", *Structural Stability and Design,* Kitipornchai, Hancock and Bradford (Eds), Balkema, Rotterdam, 55-60.
Zhao, X.L., Mckinlay, G., P. Lim, P. Joseph and Pi, Y.L. (1997), "Structural behaviour of a space frame utilising the oktalok nodal connection system", *Australian Civil/Structural Engineering Transactions*, IEAust., **CE39**(1), 35-41.